Response to referee comments

Referee comments 1#

Summary/recommendations:

This is an interesting paper that provides a generally clear and thorough analysis of particulate-phase MSA in the Ross Sea region. The authors have done an excellent job presenting several different results that provide a clear picture of MSA-containing particles in this region for particles between ~0.1-2 μm. I particularly appreciated their discussions upon why MSA condenses on some particle types but not others. This study can become a useful resource to the community. However, there were details missing in the methods that made a complete evaluation of this study difficult. My primary concern is that the authors did not make it clear whether the datasets were screened for ship exhaust (pollution) contamination. If this was not done, the results would likely be skewed, in particular those that discuss particle speciation. I have outlined a few other concerns in my review below. If the authors have corrected their data for ship contamination and simply didn't include these details in the manuscript, then I recommend that this study be published after the revisions discussed below. If the authors have not corrected their data for ship contamination, then I request either evidence that ship contamination was not a problem during the entire study, or that the data be corrected and reanalyzed.

Thanks very much for the comments. The shipboard observation is a challenge and specifically in the marine environment. It is the case that ship emissions may impact the observation data. In this study, to minimize the impact of self-contaminations of the vessel on the observation results, the air inlet connecting to the monitoring instruments is fixed to a mast at 20 meters above the sea surface located at the bow of the R/V. Note that the major pollution source is from the chimney, which is located at the stern of the R/V and about 25 meters above the sea level. Hence, the pollution emissions from the vessel mainly located at the downwind of the sampling inlet, especially when the vessel is running. As high-time-resolution observations are used in this study, the self-contaminations from the vessel have been eliminated from the measurement results. The wind speeds and wind directions were also monitoring during the observation period, which were used to determine if the observations were affected by the self-contaminations or not in this study. The data has been corrected to eliminate the impact of ship contaminations in this study.

General comments:

The paper should be edited throughout for grammar. The authors use tense in confusing ways--they often use past tense when present tense is more appropriate and clear. For example, Lines 43-44: "The chemical components and sources of aerosol particles in the marine atmosphere were rather complicated" (italics mine). The chemical components and sources are still complicated, and the present tense should be used here. Please check tense use throughout. As well, verb endings are often incorrect. For example, line 25: "... deriving from the oxidation…". This should be "derived" here.

Thanks for the suggestion, we have revised the tense throughout the manuscript.

Define the size ranges meant by 'fine particles' and 'coarse particles' in this paper. Different studies use different definitions.

In this study the size range of 'fine particles' is from 0.1 to 2.0μm, seen in line 98 in the revised manuscript. Size range of 'submicron particles' is 0.1-1.0μm (line 243 in the revised manuscript), and the size range of 'coarse particles' is from 1.0 to 2.0μm (line 244 in the revised manuscript). We have added the definition in the manuscript.

The authors must define each acronym when it is first used. For instance, MP1 and MP2 are brought up in lines 139-144 but are not explained or defined. Same for 'MA' (line 148).

MP1 and MP2 represent the high MSA population regions (line 144-145), MA represents the high MSA mass region (line 152). We have added the description in the manuscript.

There needs to be discussion in the methods of:

--Particle size range of the IGAC and SPAMS. In the results, there is mention that particles between .1-2.5 μm were considered from the SPAMS. Is this the size range used throughout the study? Not being able to capture particles <100 nm is a limitation of this study and should be acknowledged and discussed.

The measurement particle size range of ~10μm for IGAC, and 0.1~2.5μm for SPAMS. It is true that particles smaller than 100nm cannot be detected by the SPAMS in this study. Note that most of the MSA particles were in the range of 0.1 to 1.0μm in the marine atmosphere (Ayers et al., 1997), indicating that the MSA particles measured in this study represent most of the MSA particles in the marine atmosphere. We have added the discussion in the manuscript (line 328-331).

--Very important: how the authors corrected for potential contamination of pollution from the ship. Although pollution from the ship likely wouldn't impact the MSA measurements, it would impact the total aerosol population and mass concentrations. As well, contamination from ship pollution could alter the speciation of the particles, skewing the authors' results. Did the authors exclude time periods in which the ship pollution would have impacted the measurements?

As mentioned above, to minimize the impact of self-contaminations of the vessel on the observation results in this study. The following methods were used: 1) The air inlet connecting to the monitoring instruments was fixed to a mast at 20 meters above the sea surface located at the bow of the R/V. Note that the major pollution source is from the chimney, which is located at the stern of the R/V and about 25 meters above the sea level. Hence, the pollution emissions from the vessel mainly located at the downwind of the sampling inlet, especially when the vessel was running. 2) The wind speeds and directions were also monitored during the observation period, which were used to determine if the observations were affected by the self-contaminations or not in this study. 3) As high-time-resolution observations were used in this study, the self-contaminations from the vessel were eliminated from the measurement results, seen in line 77-80.

In this study, the NO_x concentration was also monitored simultaneously during the cruise (Fig. SS1). The NO_x concentrations were extremely low and remained stable in this study, indicating that the sampling gases were rarely affected by the ship emissions. We have checked the data when high NO_x concentrations were present. The data have been excluded, when the observations were impacted by the ship pollution in this study.

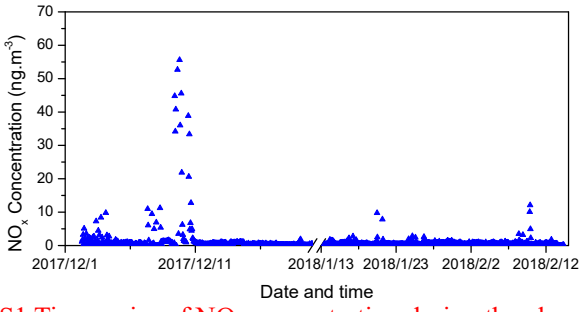

Fig. SS1 Time series of NO_x concentration during the observation

--Length of the tubing used for sampling and whether there were corrections for particle and vapor losses within the tubing and associated uncertainties.

The length of the tubing is about 20 meter. It is true that the particle and vapor would lose in the tubing. In this study, conductive silicon tubing was used to minimize the particle lost in the tubing. A high velocity sampling system was also used in this study with a gas velocity of about 4.25m/s in the tubing. The residence time of the gases in the tubing is about 4.7 seconds. The measurements of aerosol particles with and without the tubing have been carried out. There are few differences between the measuring results with and without the tubing. Hence, the particle and vapor losses in the tubing can be neglected in this case.

Line 125: ‘and their populations’ is confusing here. I see later in the text that particle populations are determined by the SPAMS. Please make that clear here.

We have added the revised in the manuscript (line 127 in the revised manuscript).

Lines 145-147: The authors provide the MSA particle population. It would be of interest to provide the total particle population as well, for comparison. I see this comparison is made in section 3.3; perhaps the authors can refer the reader to that section for comparisons of MSA-containing particles to the total particle concentration.

Thanks for the suggestion, we have added the notice to refer the reader to the section for comparisons of MSA-containing particles to the total particle concentration, seen in line 151-152.

Sections 3.3.1-3.3.7: For consistency and to provide a complete picture for each speciation, I suggest briefly including results from Figs 4 and 5 for each species subtype. Figs 4 and 5 are currently inconsistently discussed between sections. (For example, provide the mean fraction that each subtype contributes to the total population [Fig 4] within each section and so forth.) The authors are not limited by space for this journal, and this discussion is currently unsatisfying.

Thanks for the suggestion. In this study, we focused on the characteristics of MSA particles, hence, we did not discuss other species in this manuscript to make the manuscript clear and concise. Here, we provided the complete picture for each speciation in the SI (seen in Fig. S6). The mean fraction of each subtype contributes to the total population during leg I and leg II are also illustrated in the SI (seen in Fig. S8). We have added the discussion in this section to smooth the discussion between Fig 4 and Fig. 5, seen in 320-331 in the revised manuscript.

Section 3.3.7: discuss sources of NOx, HNO_3 in the marine atmosphere here

We have added the discussion of NO_x, HNO_3 sources in the marine atmosphere in section 3.3.7, seen in line 280-285.

Figures/tables:

Supplemental figures are not currently referenced in order in the main text. For instance, lines 68-72 jump from Figure S1 to Figure S4. Please update the SI figures to reflect the order they are referenced in the text.

We have updated the Figure order in SI.

Figure 3: it is very hard to read the speciation (Na+, C 4 H, etc) on each mass spectra plot. I recommend increasing the font size, if possible.

We have increased the font size in Figure 3.

Figure 4: It is very hard to read the legends on this plot. I highly recommend increasing the font size; there is likely enough space to make each legend into 2 columns. As well, the percents in the pie chart are difficult to read.

We have enlarged the legend and the percents in the pie chart in Figure 4.

Figure S4: There need to be units on the colorbars for sea ice coverage (presumably percent) and Chl-a. As well, the units can be included in the figure caption (that should be updated to Fig. S4 instead of Fig. 4).

We have revised in the Figure S4 in the SI.

Figure 6. I quite like this schematic; all of the text could be larger for clarity.

Thanks very much, we have enlarged the text size in the Figure 6.

Technical comments:

I suggest defining ‘polynya’ the first time it’s mentioned in the abstract and main text, as it is not a common term.

‘polynya’ is defined as an area of open sea water surrounded by ice. We have added the definition of ‘polynya’ in the abstract (line 12) and main text (line 58).

Line 11: change to “lacking in knowledge”

We have changed in line 11.

Lines 17-18: do the authors mean that MSA uptake favored sea salt particles? Suggest rewording.

We have revised in the manuscript (line 18-19).

Line 104: W should be capitalized and there is a missing negative in the denominator of ‘W/cm -2 ’

We have revised in the manuscript (line 106).

Line 116: ‘cloud effect’ is confusing, I suggest rewording. I assume the authors are referring to the loss of data due to clouds?

It is the case that the satellite data of Chl-a is affected by the clouds, resulting in the loss of data. We have revised in the manuscript (line 118).

Line 119: please define ‘centration data’

We have checked the information. This is a typo here. It is ‘ We used the sea ice concentration data from the daily…’. (line 121)

Line 179: Do the authors mean “was consistent” instead of “consisted”?

We have changed in the manuscript (line 185).

Line 278: do the authors mean ‘species’ rather than ‘particles’?

For SPAMS detection, particle is determined individually to provide single particle chemical compositions and size. Hence, different types of particles can be identified (such as Na, Mg, SO_4^{2-} etc.). Here, we obtained the particle count of different types of particle but did not the particle mass concentration with SPAMS. Hence, ‘particles’ was used here.

Line 284: the word ‘except’ here is confusing. It is unclear to me what the authors intend by this statement.

Here we mean that the particle population was not the only impact factor for the uptake of MSA (line 298-299). We have revised in the manuscript.

References:

Ayers, G.P., Cainey, J.M., Gillett, R.W., Ivey, J.P. Atmospheric sulphur and cloud condensation nuclei in marine air in the Southern Hemisphere, Phil. Trans. R. Soc. Lond. B, 1997, 352, 203-211

Referee comments 2#

Summary:

The manuscript "Uptake selectivity of Methanesulfonic Acid (MSA) on fine particles over polynya regions of the Ross Sea, Antarctica" presents results form a field campaign undertaken in 2017/2018. The focus of this study is to investigate the uptake of MSA on different particle types. For this purpose MSA mass concentrations and total aerosol population, coupled with size resolved data, were collected simultaneously. The results of this study provide a clear characterization of MSA uptake in the presence of different pre-existing particles, which I believe is of high interest for the aerosol community. Therefore, I recommend the paper for publication after the following comments have been addressed:

Major comment:

I think the results are described in a very clear and precise way. The only thing I was wondering about is the probability of the source of certain particles. It is discussed that Na and Mg are typically associated with sea spray aerosols, while EC and OC are more associated with primary emissions from combustion processes and K with biomass burning. Did the authors try to check where the air-masses were originating from during the campaigns to assess whether biomass-burning or in general combustion processes would have been expected during this period? If there were no known sources of such processes during this time–could this indicate that the pre-existing particles originated from long-range transport? I would recommend to include a discussion on this in the revised manuscript.

It is true that aerosol particles would be impacted by the long-rang transport sources. The back trajectories along the cruise tracks in Ross Sea are given in the Fig. SS2. The major air masses originated from the local sources during the cruise. The aerosol particle chemical compositions did not reveal an obvious correlation with air back trajectories in this study (Fig. 4 and Fig. SS2). Hence, in this study, particles were mainly associated with the local sources but not the long-range transport.

OC particles are often associated with anthropogenic sources, such as vehicle and coal combustion (Silva et al., 2000; Stiaras et al., 2008), marine biogenic sources (Quinn et al., 2014) and secondary sources (Horne et al., 2018). It is the case that OC particles are mainly derived from fossil fuel combustion and secondary sources in the coastal and urban regions. But in the marine atmosphere, OC particles are often determined by the marine biogenic sources (Quinn et al., 2014, Yan et al., 2018). EC particles are typically associated with primary emissions from fossil fuel combustion, such as ship emissions in the ocean area. K is often used as a marker of biomass burning in the continent, but K can also be derived from other sources, such as coal combustion, biological materials. In this study, the signature of K is very different from the K signature from biomass burning, indicating that K particles are not associated with the biomass burning. Na and Mg are often associated with sea salt particles in the marine atmosphere. Positive corrections between Na, Mg and wind speeds are present in the Fig. SS3, indicating that those particles are derived from sea spray aerosols.

We have added the discussion in the manuscript, seen in section 3.3.1-3.3.7.

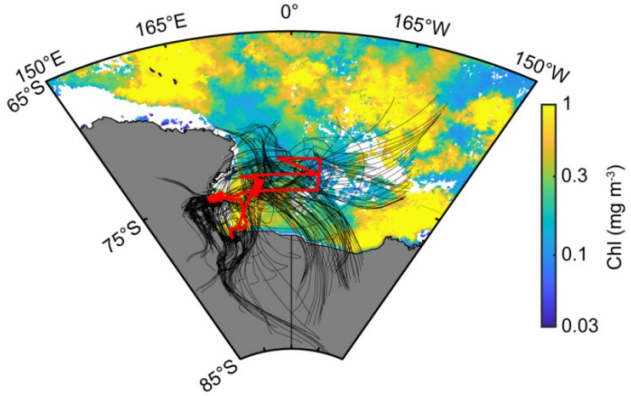

Fig. SS2 The back trajectories along the cruise tracks in Ross Sea

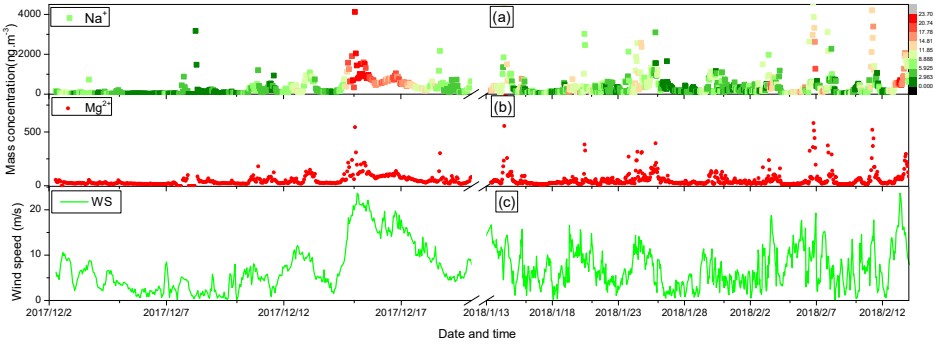

Fig. SS3 Time series of Na and Mg concentrations and wind speeds during the cruise.

Minor comments:

1. The manuscript currently presents data described in a mixture of present and past tense. I recommend sticking to one tense throughout the manuscript.

Thanks for the suggestion, present tense is accepted. We have revised throughout the manuscript.

2. The manuscript contains several mistakes regarding singular/plural expressions that should be revised.

We have revised in the manuscript.

3. It is stated in the manuscript that sea spray aerosols generated by bursting bubbles are generally in the course mode (page 15, lines 322-323). This is not correct as the majority of particles form bubble busting (considering number concentrations) peak at diameters around 100 nm. See for example De Leeuw et al. (2011) or Prather et al. (2013).

It is the case that sea spray aerosols peak at diameters around 100 nm in some studies (De Leeuw et al. (2011) or Prather et al. (2013)), and the major sea spray aerosols are in submicron size (number concentrations). But the sea salt particles have a wide size distribution, ranging from 0.01-8 μm (Clarke et al., 2006). The expression is ambiguous here. We have revised in the manuscript (line 348-349). Thanks for the suggestion.

Specific comments:

Page 2, line 38: replace “have showed” with “have shown”

We have revised in the manuscript, seen in line 38.

Page 2, line 43: replace “were” with “are”

We have revised in the manuscript, seen in line 43.

Page 3, line 64: replace “intensity” with “intense”

“intense” is accepted in the manuscript, seen in line 63.

Page 3, lines 71-72: replace “ices” with “ice” Line 72: As an example of the “minor comment 1”: replace “have” with “had”

We have revised in the manuscript.

Page 5, line 104: use a capital “W” for the unit “Watt”

We have revised in the manuscript, seen in line 106.

Page 6, line 139: remove the “the” in front of “leg I”.

The “the” has been removed in the manuscript.

Page 6, line 414: replace “following” with “followed”

The “followed” is accepted in the manuscript.

Page 7, line 158: replace “were presented” with “were present”; this mistake occurs more often in the manuscript.

We have revised throughout the manuscript.

Page 8, line 180: I am not sure I would call a R^2=65 a “strong positive correlation”, rather just a “positive correlation”

“positive correlation” is appropriate here, line 186.

Page 10, line 232: Rephrase the beginning of the sentence – “The simultaneous...”

We have rephrased in the manuscript, seen in 239-241.

Page 11, line 234: Replace “suggesting” with “suggest”

We have revised in the manuscript, seen in line 241.

Page 11, line 235: Add “c,d” to the citation of the figure 5

We have added “c,d” to the citation of the Figure 5, seen in line 242.

Page 11, line 251: rephrase “a few signals of..”

We have revised in the manuscript, seen in line 260.

Page 12, line 257: example of “minor comment 2”: replace “were” with “was”

We have revised in the manuscript, seen in line 266.

Page 14: line 299: replace “conforming” with “confirming”

We have revised in the manuscript, seen in line 314.

Page 17: line 350: rephrase sentence starting with “The other one halogen radicals...”

We have revised in the manuscript, seen in line 375-377.

Page 17: line 364: rephrase sentence starting with “Following by the MSA-Na...”

We have rephrased in the manuscript, seen in line 388.

Page 17: lines 369-371: Delete last sentence as it is repeated in the conclusion.

We have deleted the sentence in the manuscript.

We tried our best to improve the manuscript and revised carefully to improve the manuscript. Here we did not list the minor changes but marked in red in the revised paper. We appreciate for Editors/Reviewers’ warm work earnestly, and hope that the correction will meet with approval. Once again, thank you very much for your comments and suggestions.

References:

De Leeuw, G., Andreas, E. L, Anguelova, M. D., Fairall, C. W., Lewis, E. R., O’Dowd, C., Schulz, M., and Schwartz, S. E. (2011), Production flux of sea spray aerosol, Rev Geophys., 49, RG2001, doi:10.1029/2010RG000349.

Prather, K.A., T.H. Bertram, V.H. Grassian, G.B. Deane, M.D. Stokes, P.J. DeMott, L.I. Aluwihare, B.P. Palenik, F. Azam, J.H. Seinfeld, R.C. Moffet, M.J. Molina, C.D. Cappa, F.M.Geiger,G.C.Roberts,L.M.Russell,A.P.Ault,J.Baltrusaitis,D.B.Collins,C.E.Corrigan, L.A. Cuadra-Rodriguez, C.J. Ebben, S.D. Forestieri, T.L. Guasco, S.P. Hersey, M.J. Kim, W.F. Lambert, R.L. Modini, W. Mui, B.E. Pedler, M.J. Ruppel, O.S. Ryder, N.G. Schoepp, R.C. Sullivan, and D. Zhao (2013). Bringing the ocean into the laboratory to probe the chemical complexity of sea spray aerosol. PNAS, 110(19):7550– 7555.

Clarke, A. D., Owens, S. R. Zhou, J. An ultrafine sea-salt flux from breaking waves: implications for cloud condensation nuclei in the remote marine atmosphere. J. Geophys. Res. 111, D06202. (doi:10.1029/2005JD006565), 2006.

Silva, P. J., Carlin, R. A., Prather, K. A. Single particles analysis of suspended soil dust from Southern California. Atmos. Environ. 34, 1811-1820, 2000.

Sitaras, I. E., Siskos, P. A. The role of primary and secondary air pollutants in atmospheric pollution: Athens urban area as a case study. Environ. Chem. Lett. 6, 59-69, 2008.

Horne, J.R., Zhu, S., Montoya-Aguilera, J., Hinks, M.L., Wingen, L.M., Nizkorodov, S.A., Dabdub,D. Reactive uptake of ammonia by secondary organic aerosols: Implications for air quality. Atmos. Environ. 189, 1-8, 2018.

Quinn, P.K., Bates, T.S., Schulz, K.S., Coffman, D.J., Frossard, A.A., Russell, L.M., Keene, W.C., Kieber, D.J. Contribution of sea surface carbon pool to organic matter enrichment in sea spry aerosol. Nature Geos. 7, 228-232, 2014.

Yan, J., Lin, Q., Zhao, S., Chen, L., Li, L. Impact of marine and continental sources on aerosol characteristics using an on-board SPAMS over Southeast Sea, China. Environ. Sci. Pollution Res. 25, 30659-30670, 2018.

List of all relevant changes in the manuscript

1. Line 12, Add the definition of polynya (an area of open sea water surrounded by ice).

2. Line 57-58, Add the definition of polynya (an area of open sea water surrounded by ice).

3. Line 77-78, Add the discussion about the self-contaminations from the vessel and how to exclude the pollution from the ship emissions.

4.Line 85-86, Add the detection particle size of IGAC.

5.Line 98, Add the description of fine particle size.

6.Line 144-145, Add the definition of MP.

7.Line 153, Add the definition of MA.

8.Line 243-244, Add the definition of size ranges of submicron particles and coarse particles.

9.Line 250-253, Add the discussion about sources of K particles.

10.Line 265-267, Add the discussion about sources of EC particles.

11.Line 280-285, Add the discussion about sources of NO_x^- in the marine atmosphere.

12.Line 320-331, Add the discussion about the linkage between Fig.4 and Fig.5.

13. Line 348-349, Add the descriptions of sea salt particle size.

Uptake selectivity of Methanesulfonic Acid (MSA) on fine particles over polynya regions of the Ross Sea, Antarctica

Jinpei Yan[*1,2], Jinyoung Jung[3], Miming Zhang[1,2], Federico Bianchi[4], Yee Jun Tham[4], Suqing Xu[1,2], Qi Lin[1,2], Shuhui Zhao[1,2], Lei Li[5], Liqi Chen[1,2]

1 Key Laboratory of Global Change and Marine-Atmospheric Chemistry, MNR, Xiamen 361005, China;

2 Third Institute of Oceanography, Ministry of Natural Resources, Xiamen 361005, China;

3 Korea Polar Research Institute, 26 Songdomirae-ro, Yeonsu-gu, Incheon 21990, Republic of Korea；

4 Institute for Atmospheric and Earth System Research; University of Helsinki, 00014, Finland;

5 Institute of Mass Spectrometer and Atmospheric Environment, Jinan University, Guangzhou 510632, China

Abstract: The uptake of methanesulfonic acid (MSA) on existing particles is a major route of the particulate MSA formation, however, MSA uptake on different particles is still lack in knowledge. Characteristics of MSA uptake on different aerosol particles are investigated in polynya (an area of open sea water surrounded by ice) regions of the Ross Sea, Antarctica. Particulate MSA mass concentration, as well as aerosol population and size distribution, are observed simultaneously for the first time to access the uptake of MSA on different particles. The results show that MSA mass concentration does not always reflect MSA particle population in the marine atmosphere. MSA uptake on aerosol particle increases the particle size and changes aerosol chemical composition, but does not increase the particle population. The uptake rate of MSA on particle is significantly influenced by aerosol chemical properties. Sea salt particles are beneficial for MSA uptake, as MSA-Na and MSA-Mg particles are abundant in the Na and Mg particles, accounting for 0.43±0.21 and 0.41±0.20 of the total Na and Mg particles, respectively. However, acidic and hydrophobic particles suppress the uptake of MSA, as MSA-EC and MSA-SO_4^{2-} particles account for only 0.24±0.68 and 0.26±0.47 of the total EC and SO_4^{2-} particles, respectively. The results extend the knowledge of the formation and environmental behavior of MSA in the marine atmosphere.

Keywords*:* Methanesulfonic acid (MSA); nss-SO_4^{2-}; aerosol; climate change; Antarctica

1. Introduction

*Corresponding author. Tel.: +86 592 2195370; Fax: +86 592 2195280, E-mail address: jpyan@tio.org.cn; Address: No.178 Daxue Road, Siming district Xiamen, Third Institute of Oceanography, MNR, 361005, P R China.

Methanesulfonic acid (MSA) and non-sea-salt-sulfate (nss-SO_4^{2-}), derived from the oxidation of dimethyl sulfide (DMS), are important sources of cloud condensation nuclei (CCN) in the marine boundary layer (Chang et al., 2011; Ghahremaninezhad et al., 2016). Different from nss-SO_4^{2-}, MSA is exclusively from the oxidation of DMS in the atmosphere (Sorooshian et al., 2007). Thus, MSA is expected as a useful marker for the deconvolution of sulfate from marine biogenic and non biogenic sources (Legrand et al., 1998).The ratio of MSA to nss-SO_4^{2-} is often used to assess the DMS oxidation routes and the contributions of biogenic sulfur to other sulfur sources (Sorooshian et al., 2007; Wang et al., 2014). DMS oxidation routes, as well as the products of MSA and nss-SO_4^{2-}, have been investigated previously in the marine atmosphere (Preunkert et al., 2008; Kloster et al., 2006).

Generally, particulate MSA is generated from the reactive uptake of DMS and condensation of gaseous MSA on aerosol particles (Davis et al., 1998; Barnes et al., 2006). A recent study shows that MSA can increase sulfate cluster formation rate by up to one order of magnitude, increasing the stability of the clusters (Bork et al., 2014). However, previous studies have shown that SO_4^{2-} is more effective at new particle formation (NPF) than MSA, while MSA is more likely to condense onto existing particles (Hayashida et al., 2017). Although the reactive uptake of MSA on fine particle has been demonstrated in the previous studies (Sorooshian et al., 2007; Bates et al., 1992), the influence of aerosol characteristics on MSA uptake is not present.

The chemical components and sources of aerosol particles in the marine atmosphere are still complicated (Weller et al., 2018). Filtered sample methods were often used in previous studies (Jung et al., 2014; Preunkert et al., 2007; Read et al., 2008) with a long sampling interval to accommodate the detection limit of the instrument (Preunkert et al., 2007; Zhang et al., 2015). It is, therefore, difficult to clarify how MSA mixes with other aerosol species, using bulk aerosol sampling methods, as only mean aerosol chemical components are obtained during the sampling period (Bates et al., 1992; Chen et al., 2012). On-line aerosol mass spectrometry has been used to characterize the aerosol chemical species and sizes with high-time-resolution (Yan et al., 2018; Healy et al., 2010), allowing the determination of particle mixing states and sources. Although a few studies show that MSA is often associated with Mg in aerosol particles, probably due to marine biogenic activity (Casillas-Ituarte et al., 2010), studies of the interactions between MSA

and other aerosol species are still rare. Theoretical and laboratory studies have attempted to explain these observations and determine in which way MSA enters aerosol particle (Bork et al., 2014). However, the relative likelihood of MSA uptake on different particles remains uncertain.

In this study, we examined the uptake characteristics of MSA on different particles over polynya (an area of open sea water surrounded by ice) regions in the Ross Sea (RS), Antarctica, based on high-time-resolution observations. MSA mass concentrations and particle populations, as well as aerosol compositions and size distributions, were measured simultaneously for the first time in the RS using an in-situ gas and aerosol compositions (IGAC) and a single particle aerosol mass spectrometer (SPAMS) monitoring instrument. Observations were carried out in two different seasons, the early December with intense sea ice coverage and in the mid-January to February with sea ice free in the RS.

2. Experiment methods and observation regions

The observations were carried out on-board of R/V "Xuelong", covering a large region of the RS, Antarctica (50°S to 78°S, 160°E to 185°E) (Fig. S1) with different sea ice concentrations. The leg I was carried out from December 2 to 20, 2017. The sea surfaces were covered with intense sea ice in the RS during this period (Fig. S2a). However, when we arrived back in the RS (leg II, from January 13 to February 14, 2018), the sea ice had almost melted in the RS (Fig. S2b).

2.1 Observation instruments and sampling inlet

An in-situ gas and aerosol compositions monitoring system (IGAC, Model S-611, Machine Shop, Fortelice International Co., Ltd., Taiwan; http://www.machine-shop.com.tw/), and a single particle aerosol mass spectrometer (SPAMS, Hexin Analysis Instrument Co., Ltd.) were used to determine aerosol water-soluble ion species, particle size distributions and chemical compositions, respectively (Fig. S3). The sampling inlet connecting to the monitoring instruments was fixed to a mast 20 meters above the sea surface to minimize the impact of self-contaminations of the vessel.

Wind speeds and directions were also monitored during the cruise. The observation period in which self-contaminations impacted the measurement have been excluded based on the high-time-resolution observation data. A total suspended particulate (TSP) sampling inlet was positioned at the top of the mast. Conductive silicon tubing with an inner diameter of 1.0 cm was used to make the connection to all instruments.

2.2 Aerosol water-soluble ion species

Gases and aerosol water-soluble ion species were determined using a semi-continuous IGAC monitor. A PM_{10} cyclone was conducted for the IGAC sampling, hence, the measurement particle size is ~10μm of the IGAC in this study. Gases and aerosols are separated and streamed into a liquid effluent for on-line chemical analysis at an hourly temporal resolution (Young et al., 2016; Liu et al., 2017). The analytical design and methodology for the determination of gases and aerosol water-soluble ions have been described in detail by Tao (2018) and Tian (2017). Fine particles are firstly enlarged by vapor condensation and subsequently accelerated through a conical-shaped impaction nozzle and collected on the impaction plate. The samples are then subsequently analyzed for anions and cations by an on-line ion chromatography (IC) system (DionexICS-3000). The injection loop size is 500 μL for both anions and cations. Six to eight concentrations of standard solutions are selected for calibration, depending on the target concentration, in which the R^2 was above 0.997 (Fig. S4). The detection limits for MSA^-, SO_4^{2-}, Na^+, and Cl^- are 0.09, 0.12, 0.03, and 0.03 μg/L (aqueous solution), respectively.

2.3 Aerosol size distribution and chemical compositions

The detection method for fine particles (0.1-2.0 μm) using a SPAMS has been described in detail by Li (Li et al., 2011; Li et al., 2014). Particles are introduced into the vacuum system through a critical orifice, then focused and accelerated to form a particle beam with specific

velocity. The particle beam passes through two continuous diode Nd: YAG lasers (532 nm), where the scattered light is detected by two Photomultiplier Tubes (PMTs). The velocity of a single particle is then determined and converted into its aerodynamic diameter. The individual particle is ionized with a 266 nm Nd: YAG laser to produce positive and negative ions. The fragment ions are analyzed using a bipolar time-of-flight mass spectrometer. The power density of the ionization laser is kept at 1.56×10^8 $W.cm^{-2}$.

The particle size data and mass spectra are analyzed using the YAADA software toolkit (http://www.yaada.org/) (Allen 2005). An adaptive resonance theory based neural network algorithm (ART-2a) is applied to cluster individual particles into separate groups based on the presence and intensity of ion peaks in the single particle mass spectrum (Song et al., 1999), with a vigilance factor of 0.65, a learning rate of 0.05, and a maximum of 20 iterations.

2.4 Metrological data

Meteorological parameters such as temperature, humidity, wind speed, and direction were measured continuously using an automated meteorological station deployed in the R/V "Xuelong", which was located on the top deck of the vessel.

2.5 Satellite data of sea ice and chlorophyll-a

In this study, we used remote sensing data to show the spatial and temporal distribution of chlorophyll and sea ice concentrations in the RS. To reduce the impact of cloud and swath limits, we chose the 8-day datasets for the remote sensing of chlorophyll-a from MODIS-Aqua (http://oceancolor.gsfc.nasa.gov) with a spatial resolution of 4 km. We used the sea ice concentration data from the daily 3.125-km AMSR2 dataset (Spreen et al., 2008) (available at https://seaice.uni-bremen.de). Each grid of the gridded datasets with a sea ice concentration less than or equal to 15 % was regarded as comprising all water (Cavalieri et al., 2003). The time series of the total regional mean value in the study region was then plotted.

3. Results and discussion

3.1. Spatial distributions of MSA mass concentration and particle population

MSA mass concentrations were measured continuously in the RS. The spatial distributions of MSA mass concentrations and particle populations in Fig. 1 are created with Ocean Data View (Schlitzer 2015; Schlitzer et al., 2002). MSA concentrations range from 14.6 to 210.8 ng.m^{-3}, with an average of 43.8±22.1 ng.m^{-3} during leg I (Fig.1a), consisting with summertime MSA levels recorded at Halley station (75°39'S, with an average of 35.3 ng.m^{-3}) and Dumont d'Urville station (66°40'S, with an average of 49 ng.m^{-3}) (Minikin et al., 1998), but lower than those reported at Palmer station (64°77' S, with an average of 122 ng.m^{-3}) (Savoie et al., 1993). The highest MSA levels occur at the region (64° - 67° S), with an maximum value of 210.8 ng.m^{-3} (Fig. 1a), consisting with the previous observation results obtained from the Southern Ocean (60 - 70° S; maximum MSA level of 260 ng.m^{-3}) (Chen et al., 2012). In this study, elevated MSA levels are associated with the dynamic sea ice edge at ~64° S, as sea ice starts to melt in the early December (Fig. S2a and Fig. S2c). The release of iron (De Baar et al., 1995; Wang et al., 2014) and algae (Lizotte et al., 2001; Loose et al., 2011) from sea ice increase phytoplankton numbers (Taylor et al., 2013), resulting in the increase of DMS generation and emission (Hayashida et al., 2017). This, in turn, increases MSA levels due to the oxidation of DMS in the atmosphere.

MSA particle populations (0.1 - 2.5 μm) are determined simultaneously by SPAMS during the cruise (Fig. 1b). The highest average hourly MSA particle population (507 ± 189) occurs at MP1 (high MSA population, 68° - 72°S, 172°E) near the Antarctic continent, followed by MP2 (high MSA population, 65° - 68°S, 160° - 170° E), with an average particle population of 344 ± 334. High MSA particle populations are associated with high wind speeds in these regions (MP1 8.06 ± 1.86m/s; MP2 15.76 ± 3.93m/s; Fig. 2).

The MSA mass concentrations range from 11.4 - 165.4 ng•m^{-3} (with an average of 38.8 ± 27.5

149 ng•m^{-3}) during leg II, and the MSA particle populations range from 3 - 1666 (with an average of
150 168 ± 172; Fig. 1c and 1d). Similar variations of MSA particle population and total particle
151 population are present (Fig. 2). The relationship between MSA particle population and total
152 particle population is further discussed in section 3.2. Extremely high MSA mass concentrations,
153 with an average of 100.3 ± 18.6 ng•m^{-3}, are observed in the MA region (high MSA mass, 170.2° -
154 177.4°E, 68.2° - 77.8°S), but we do not observe high MSA particle populations in this region
155 (with an average of 171 ± 159). High MSA particle populations with low MSA concentrations
156 occur at MP1 and MP2 (Fig.1a and 1b). It indicates that MSA mass concentrations do not always
157 reflect the MSA particle populations in the marine atmosphere. Generally, the uptake of MSA on
158 aerosol surface (Read et al., 2008) only changes the aerosol size and chemical composition,
159 without varying their populations. Hence, the MSA particle population is mainly associated with
160 the aerosol number concentration in the atmosphere, as more particles are provided for the uptake
161 of MSA in high particle number concentration. Though high levels of MSA may also increase the
162 MSA population, high MSA mass concentrations with low MSA populations are observed in this
163 study. This phenomenon occurs when low existing particle populations and high MSA mass
164 concentrations are present in the marine atmosphere.

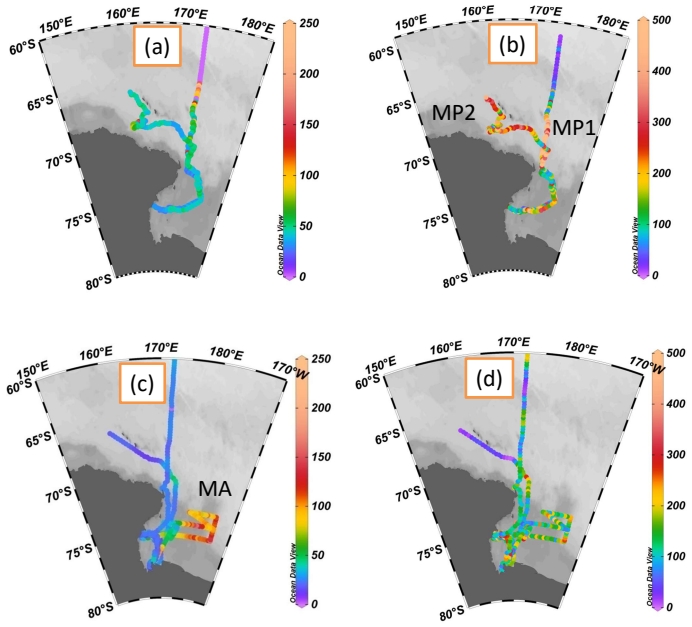

Fig.1 Spatial distribution of MSA mass concentrations and particle populations, (a) MSA mass concentrations during leg I (ng.m^{-3}); (b) MSA particle populations during leg I; (c) MSA mass concentrations during leg II (ng.m^{-3}) and (d) MSA particle populations during leg II.

3.2. Linkage between MSA concentration and particle population

To verify the relationship between MSA mass concentration and particle population, the temporal distributions of MSA mass concentration and particle number are illustrated in Fig. 2. Variations of MSA mass concentrations are not always associated with the MSA particle populations during the observation periods (Fig. 2a and Fig. 2b). We do not find an obvious correlation between MSA particle population and MSA mass concentration (Fig. S5a), indicating that the major factors regulating MSA mass concentration and MSA particle population are different. High MSA particle populations often occur in conjunction with high wind speeds (Fig. 2b and 2d), while high MSA mass concentrations are not always observed at high wind speed regions, such as extremely high MSA mass concentrations with low wind speeds are present at MA (Fig. 2a, 2b and 2d).

MSA mass concentrations are determined by the oxidation of DMS, derived from marine phytoplankton activity (Davis et al., 1998; Barnes et al., 2006; Read et al., 2008), but MSA particle populations are mainly associated with the uptake of MSA on existing particles. High existing particle populations lead to high MSA particle populations, as the formation of particulate MSA often occurs on the surfaces of existing particles (Read et al., 2008). In this study, the variation of MSA particle population is consistent with the variation of total particle population

during the observation period (Fig. 2b). A positive correlation between MSA particle population and total particle population is present (slope=0.19, r^2=0.65, n=1195, Fig. S5b). The ratio of MSA particle population to total particle population ($R_{MSA/total}$) concentrates on the range of 0.2 - 0.5, with an average of 0.29 ± 0.15 (Fig. 2b).

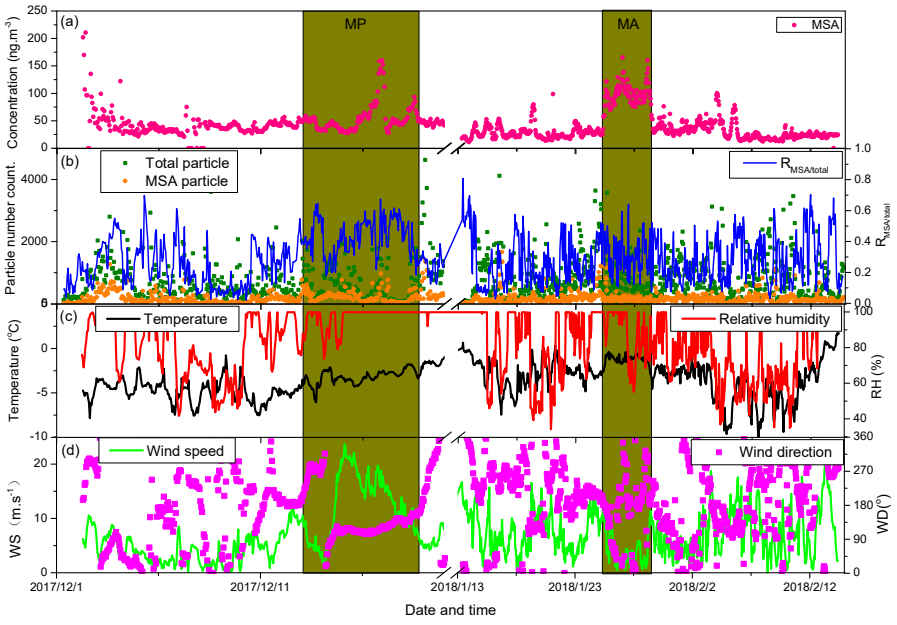

Fig. 2 Relationship between MSA mass concentration and MSA particle population in the context of various environmental factors. (a) Time series of MSA mass concentrations; (b) Time series of MSA particle population, total particle population and the ratio of MSA particle population and total particle population; (c) Time series of temperature and relative humidity (RH); and (d) Time series of wind speeds and direction.

3.3. Signatures of MSA particle types

During leg I, 332438 single particles with positive and negative mass spectra were obtained, while 603098 single particles with positive and negative mass spectra were obtained during leg II. Fine particles were classified as eight types, such as Na, Mg, SO_4^{2-}, K, EC, OC, NO_x^- and MSA, using the ART-2a algorithm (Song et al., 1999) during the cruise (Fig. S6). MSA particles account for 27.69 % and 22.08 % of the total particles during leg I and leg II, respectively. To investigate the interaction between MSA and other species, MSA particles were further classified into seven sub-types, including MSA-Na, MSA-Mg, MSA-SO_4^{2-}, MSA-K, MSA-EC, MSA-OC, and MSA-NO_x^-.

3.3.1 MSA-Na particles

Sodium, which is often associated with sea salt particles in the marine atmosphere (Teinila et al., 2014), is an important component of atmospheric aerosols in ocean regions (Yan et al., 2018). Fig. 3a illustrates the average mass spectra of MSA-Na particles during leg I and leg II. Strong Na^+ peaks with weak K^+, Ca^+, and Na_2Cl^+ peaks are observed in the positive spectrum, while strong $NaCl_2^-$ and MSA^- peaks with low Cl^-, HSO_4^-, NO_3^-, and O^- peaks are present in the negative spectrum. Similar average mass spectra for MSA-Na particles are observed during leg I and leg II, even though the two measurements are carried out under different circumstances. MSA-Na particles are the most dominant type of MSA particles, accounting for more than 30 % of total MSA particles (Fig. 4d).

3.3.2 MSA-Mg particles

Mg is another common component in ocean-derived particles, hence, such particles are often classified as sea salt particles in the marine atmosphere. However, some previous studies have shown that the chemical properties of Mg particles observed in marine environment are distinct from those of sea salt particles (Gaston et al., 2011). In this study, the mass spectral characteristics of MSA-Mg type particles include strong MSA^- and Mg peaks (Fig. 3b). In sea salt particles, the dominant peak is typically Na^+ rather than Mg^+ (Fig. 3a) due to the higher concentration of Na^+ in seawater (Guazzotti et al., 2001). Similar with MSA-Na type particles, strong Na^+ and $NaCl_2^-$ peaks with weak Cl^-, NO_3^-, K^+, and Ca^+ peaks are observed in the mass spectra, indicating that MSA-Mg type particles are also derived from sea salt particles. Strong positive correlation (r^2=0.95) between MSA-Na and MSA-Mg is present in this study (Fig. S7), indicating that these two types of particles are derived from the same sources. However, the abundance of Mg^+

fragment ion relative to Na^+ fragment ion in MSA-Mg type particles is different from MSA-Na particles, indicating that MSA-Mg particles are also affected by other sources. Studies have shown that Mg particles are correlated strongly with atmospheric DMS (r^2=0.76) (Gaston et al., 2011), indicating that Mg particles are also impacted by marine biological materials, such as cell debris or fragments, viruses, bacteria, or the organics released by lysed cells (Casillas-Ituarte et al., 2010; Gaston et al., 2011). Hence, MSA-Mg type particles are associated with both sea salt particles and biological emissions.

3.3.3 MSA-SO_4^{2-} particles

SO_4^{2-} particles are derived from different sources, such as sea salt aerosols, anthropogenic emissions, marine biogenic and volcanic sources (Legrand et al., 1998). Strong signals, peeking at m/z -97 HSO_4^- and m/z -95 MSA^-, are present in the negative spectrum (seen in Fig. 3c), consisting with previous studies with intense signals of HSO_4^- and MSA^- occurred at m/z -97 and m/z -95 (Gaston et al., 2011; Silva et al., 2000). Peaks of K^+, Na^+, Al^+, and Fe^+ are present in the positive mass spectrum and $NaCl_2^-$, NO_3^-, C_4H^- and $C_2H_2^-$ peaks are present in the negative mass spectrum, suggest that MSA-SO_4^{2-} particles are associated with different sources. This can be further demonstrated by the size distribution of MSA-SO_4^{2-} particles (Fig. 5c and 5d), as MSA-SO_4^{2-} particles are found in both submicron particles (0.1-1.0 μm) and coarse particles (1.0~2.0 μm).

3.3.4 MSA-K particles

The positive mass spectrum of the MSA-K particles is dominated by a strong K^+ peak with weak Na^+, $C_2H_3^+$ and $C_3H_7^+$ peaks (Fig. 3d). Strong HSO_4^- and MSA^- signals are present in the negative mass spectrum. Abundance of organic fragment ions are observed in the mass spectra of

MSA-K particles. K is often expected as a marker of biomass-burning source in continental areas (Yan et al., 2018). But K is also derived from other sources, such as coal combustion and biological materials. The mass spectra of MSA-K particles observed in this study are very different from the mass spectra of K particles observed from biomass burning, indicating that K particles are not associated with the biomass burning here.

3.3.5 MSA-OC particles

OC particles are often associated with anthropogenic sources, such as vehicle and coal combustion (Silva et al., 2000; Stiaras et al., 2008), marine biogenic sources (Quinn et al., 2014) and secondary sources (photochemical reaction from their precursor organic gases) (Horne et al., 2018). The positive and negative mass spectra of MSA-OC are dominated by C_xH_y ion peaks (i.e., $C_2H_3^+$, C_3H^+, $C_3H_3^+$, $C_3H_4^+$, and $C_3H_7^+$; Fig. 3e). Strong signals of HSO_4^- and MSA^- fragment ions are also present in the negative spectrum, while weak signals of Na^+ and Cl^- are observed in the positive mass spectrum (Fig. 3e).

3.3.6 MSA-EC particles

EC particles are often associated with primary emissions; that is, the incomplete combustion of carbon-containing materials (Murphy et al., 2009). In this study, MSA-EC particles are characterized by strong peaks of C_n^- (C_4^-, C_3^- and C_2^-) in the negative spectrum, while the positive mass spectrum is dominated by Ca^+ ions (Fig. 3f). EC particles are often associated with ship emissions in the ocean atmosphere (Yan et al., 2018). Compare with the average mass spectra of MSA-OC particles, the abundances of MSA^- and HSO_4^- fragment ions are lower in MSA-EC particles, indicating that the uptake of MSA on EC particles may be more difficult than the uptake of MSA on OC particles. Similar with the mass spectra of MSA-OC particles, a few fragments of

271 Na^+ and Cl^- are observed in the MSA-EC mass spectra, suggesting that MSA-OC and MSA-EC

272 particles rarely mix with sea salt particles.

273 **3.3.7 MSA-NO^-_x particles**

274 The negative spectrum of MSA-NO^-_x particle is dominated by strong peaks of MSA^-, NO_2^-,

275 and NO_3^-, with weak $C_xH_y^-$, O^-, and Cl^- peaks (Fig. 3g). Strong Na^+, $(C_3H_3^+)/K^+$, and $(C_3H_4^+)/Ca^+$

276 peaks with weak Na_2Cl^+ and CaO^+ peaks are observed in the positive spectrum. Sea salt particles

277 easily react with atmospheric HNO_3 to form nitrate and hydrogen chloride (Adachi et al., 2015).

278 The abundance of Na^+, Cl^-, and $NaCl_2^-$ ions in the mass spectra of MSA-NO^-_x particles

279 demonstrated these particles were formed by the interaction between sea salt particles and NO^-_x in

280 the marine atmosphere. Generally, NO_x^- components (NO_2^- and NO_3^-) are produced from their

281 precursor gases NO_2, N_2O and NO, mainly deriving from natural sources in the SO (Wolff, 1995)

282 and also impacted by the human activities in the coastal Antarctic regions (Mazzera et al., 2001).

283 High concentrations of NO_x^- are often found in urban atmospheric aerosols (Yan et al., 2015).

284 However, the concentrations of NO_x^- are extremely low during the whole cruise (Fig. 4),

285 indicating that NO^-_x is associated with the marine sources in this study.

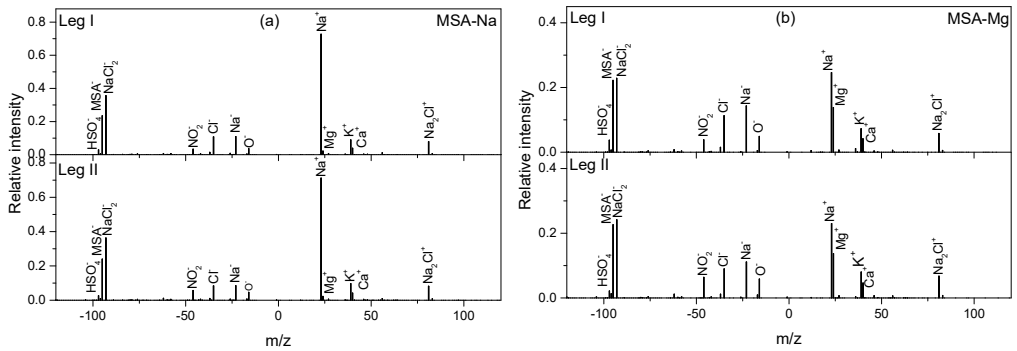

286

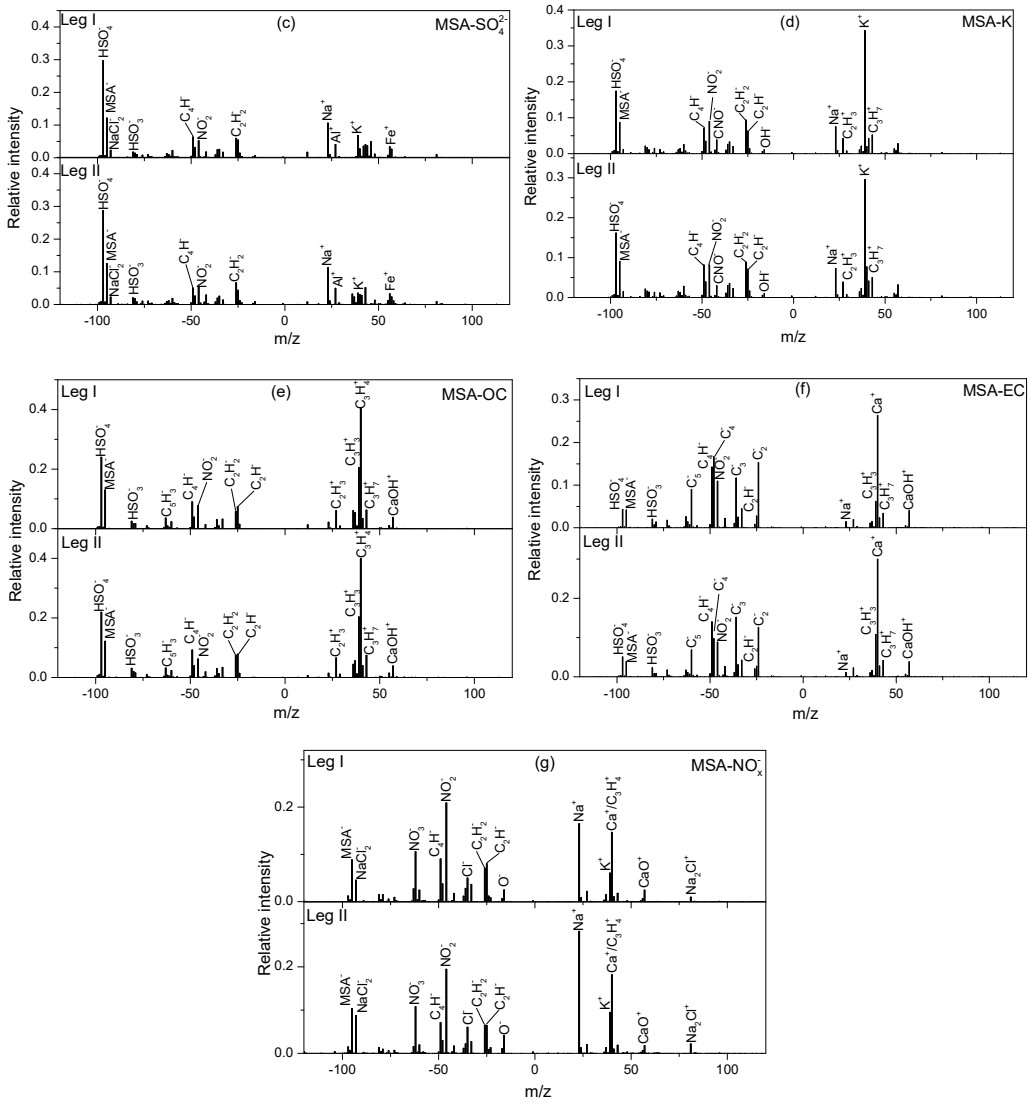

Fig. 3 Average mass spectra of major MSA clusters during leg I and leg II. (a) MAS-Na, (b) MSA-Mg, (c) MSA-SO_4^{2-}, (d) MSA-K, (e) MSA-OC, (f) MSA-EC, and (g) MSA-NO_x^-.

3.4 Uptake characteristics of MSA on existing particles

In this study, Na, Mg, and SO_4^{2-} are the most abundant particles (Fig. 4a). Similar with Na, Mg, and SO_4^{2-}, MSA-Na, MSA-Mg, and MSA-SO_4^{2-} particles are also the three most abundant MSA particles (Fig. 4b), accounting for more than 70 % of the total MSA particles. It indicates that the uptake of MSA is associated with the particle population. However, SO_4^{2-} is the most abundant particles of the total aerosol particles, while MSA-SO_4^{2-} is not the most abundant MSA particles in the atmosphere. It indicates that particle population is not the only impact factor for the uptake of MSA.

The average fractions of the MSA sub-type particles differ considerably from the average fractions of their corresponding particle types (Fig. 4c and 4d). SO_4^{2-} particles account for 26.8% of the total particles (Fig. 4c). However, MSA-SO_4^{2-} particles account for only about 17.8% of the total MSA particles (Fig. 4d). Similarly, the relative abundances of MSA-EC and MSA-K with respect to total MSA particles are lower than those of EC and K with respect to the total particles. In contrast, MSA-Na particles are the most abundant MSA particles, accounting for more than 32.55% of the total MSA particles (Fig. 4d), while Na particles account for only 21.68% of the total particles (Fig. 4c). Similar patterns are observed for Mg and OC particles. MSA-Mg and MSA-OC particles are more abundant in the MSA particles than Mg and OC particles in the total particles (Fig. 4d). These results indicate that the uptake of MSA on Na and Mg particles are more effective than the uptake of MSA on EC and SO_4^{2-} particles. Note that observations during leg I and leg II are conducted under different circumstances, as high concentrations of sea ice are present during leg I (Fig. S2a) but sea ice free occurs during leg II (Fig. S2b). Despite different conditions are present during leg I and leg II, the relative fractions of MSA sub-type particles remain similar, confirming the uptake selectivity of MSA occurs on different particles.

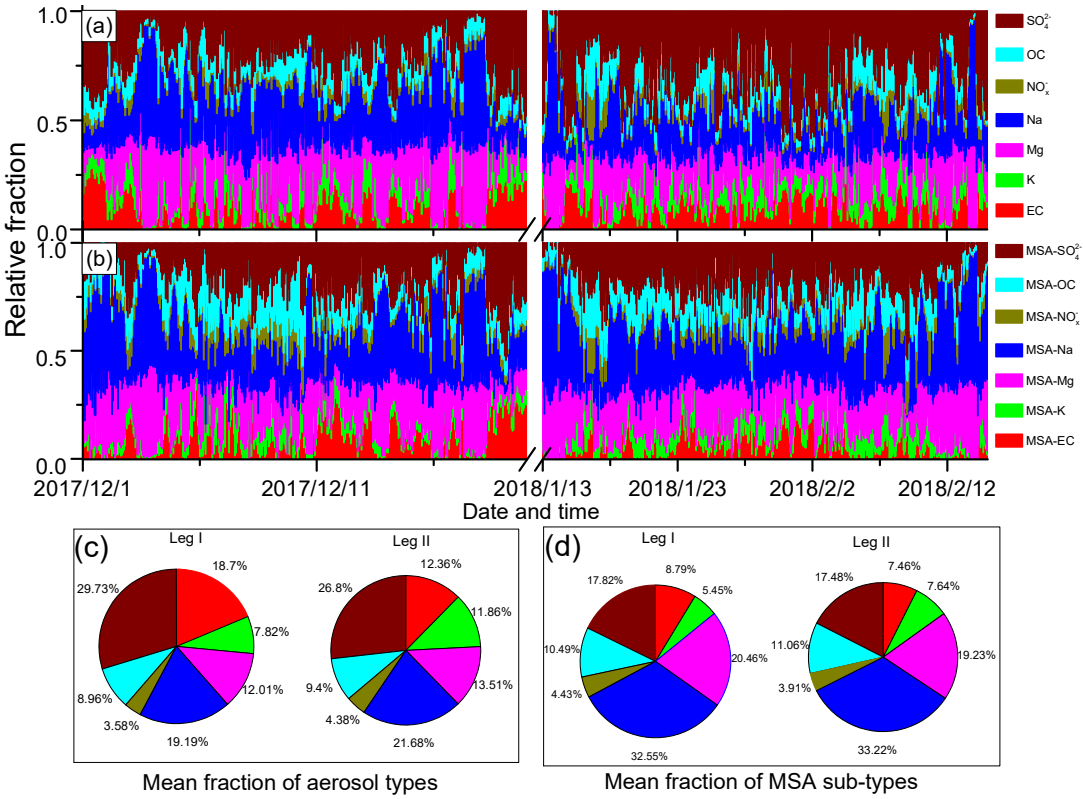

Fig. 4 Relative fractions of different particle types during leg I and leg II. (a) Relative fractions of different particle types; (b) Relative fractions of MSA sub-type particles; (c) Average fractions of different particle types during leg I and leg II; and (d) Average fractions of MSA sub-type particles during leg I and leg II.

As discussed above, relative factions of MSA sub-type particles were different from their corresponding particles. The contributions of MSA-Na and MSA-Mg to the total MSA particles are significantly improved, while the contribution of MSA-SO_4^{2-} declines. Fig. S8 illustrates the mean fractions of MSA sub-type particles to the total particle population. Similar mean fractions of MSA sub-type particles during leg I and leg II reveal that the uptake of MSA is affected by the particle chemical properties. Note that particle size also affects the uptake of MSA on fine particles. To clarify the uptake properties of MSA on different size particles, the size distributions of MSA particles (0.1-2.0 μm) and size-resolved MSA sub-type particles during leg I and leg II are also analyzed in this study. Although particles smaller than 0.1 μm cannot be detected by the SPAMS in this study, most of the MSA particles are in the range of 0.1 to 1.0 μm in the marine

atmosphere (Ayers et al., 1997), indicating that the MSA particles measured in this study represent most of the MSA particles in the marine atmosphere.

The size of the total particles shows an unimodal distribution, with a mean diameter of 0.51 μm, during leg I and leg II (Fig. 5a). Most of the particles are 0.3-1.0 μm, consisting with particle sizes observed in Antarctica using SMPS (Pant et al., 2011), and with sea spray aerosol sizes measured in marine regions (Quinn et al., 2017). Compare with mean size of the total particles, MSA particles are larger in this study, with a mean diameter of 0.65 μm (Fig. 5a). This suggests that particles are enlarged when MSA uptake occurs on their surfaces. Although particles are enlarged by MSA uptake, submicron MSA particles contribute more than 90 % of the total MSA particles (Fig. 5b), indicating that most of the MSA particles are still in the submicron range, consisting with observation results in coastal Antarctica (Legrand et al., 1998) and the Pacific Ocean (Jung et al., 2014).

The size-resolved MSA sub-type particles by population fraction during leg I and leg II are also given in this study. MSA-EC, MSA-K and MSA-NO_x^- particles are primarily distributed in small size (<1 μm) (Fig. 5c). In contrast, high relative fractions of MSA-Na and MSA-Mg particles are present in large particles (>1 μm), accounting for more than 75 % of the total coarse particles (1.0~2.0 μm) (Fig. 5c). The relative fractions of MSA-SO_4^{2-} particles do not change significantly as the particle size increases, mainly due to the variety sources of this type of particles. SO_4^{2-} particles are mainly derived from sea salt particles and the oxidation of DMS in the marine atmosphere. Sea salt particles have a wide size distribution, ranging from 0.01-8 μm (Clarke et al., 2006), which are found in submicron size (De Leeuw et al., 2011 and Prather et al., 2013) and coarse size (Norris et al., 2013). But SO_4^{2-} particles generated from the oxidation of DMS are mainly distributed in the submicron range (Legrand et al., 1998).

The MSA particle and total particle populations during leg II are much higher than during leg I (Fig. 5a) and seasonal conditions are different between leg I and leg II (Fig. S2), the size-resolved MSA sub-type particles identified during leg II are very similar with the size-resolved MSA sub-type particles identified during leg I (Fig. 5c and 5d), confirming the stable MSA uptake properties on different particles.

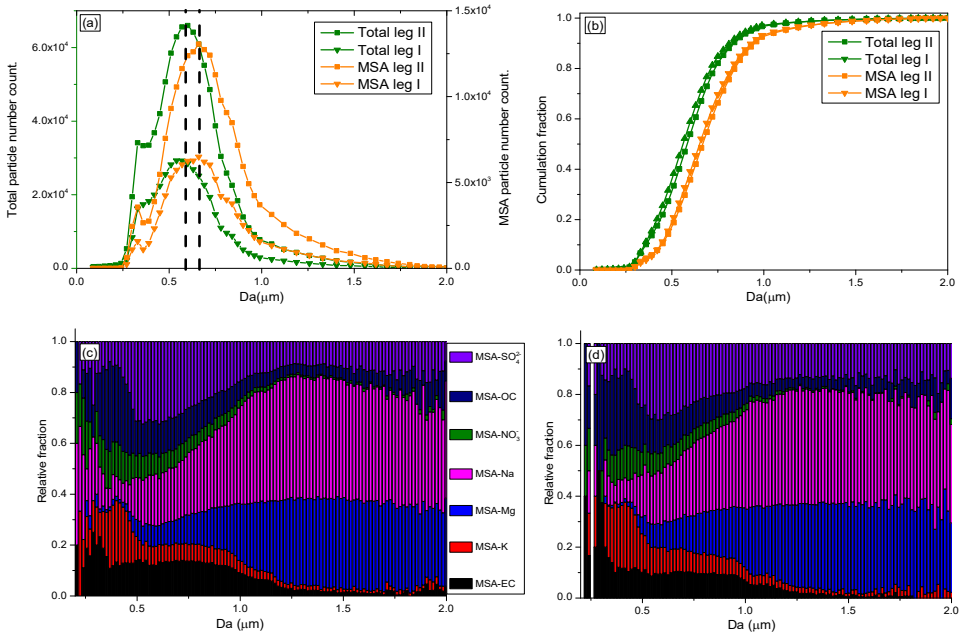

Fig. 5 Size distributions of MSA particles and size-resolved MSA sub-type particles during the cruise, (a) Size distributions of MSA particles and total particles, (b) Cumulative size distributions of MSA and total particles, (c) Size-resolved MSA sub-type particles during leg I, and (d) Size-resolved MSA sub-type particles during leg II.

3.5. The uptake rate of MSA on different particles

The uptake of MSA on the existing particles has been investigated, however, the pressing question is how different aerosol properties impact the uptake rate of MSA. Fig. 6 shows the uptake rate of MSA (defined as the ratio of MSA-containing particles to the corresponding particles, such as MSA-Na to Na ratio) on different particles in marine atmosphere. The formation of particulate MSA includes two routes, the reactive uptake of DMS on existing aerosols, and the conversion of gaseous MSA to particulate MSA by condensation on existing particles (Read et al., 2008). High uptake rates of MSA-Na and MSA-Mg particles are observed in Na and Mg particles, accounting for 0.43 ± 0.21 and 0.41 ± 0.20 of the total Na and Mg particles, respectively (Fig. 6). There are two reasons for the effective uptake of MSA on Na and Mg particles. Firstly, Na and

Mg particles are mainly derived from sea salt particles, which are often alkaline. Previous studies have shown that alkaline sea salt particles are favor to absorb acidic atmospheric gases, promoting the formation of acidic compounds on sea salt particles (Laskin et al., 2003). As an acidic species, MSA is easy to be absorbed by sea salt particles to form particulate MSA. Secondarily, the presence of halogen radicals on sea salt particle surfaces also enhance the oxidative reactive uptake of DMS on those particles to form particulate MSA (Read et al., 2008).

Low uptake rate (0.24 ± 0.68) of MSA-EC particles is observed in this study (Fig. 6). Generally, EC particles are highly hydrophobic, which suppresses the uptake of MSA on these particles, as DMS reactive uptake often occurs through aqueous reactions (Bardouki et al., 2003). The relative fraction of SO_4^{2-} particles is much higher than that of EC particles (Fig. 4c). However, the uptake rate of MSA-SO_4^{2-} particles (0.26 ± 0.47) is similar with that of MSA-EC particles (Fig. 6), indicating that particle population is not the major factor affecting MSA uptake rate. The uptake rate of MSA on existing particles is significant dependent on particle characteristics. As SO_4^{2-} particles are often acidic, MSA uptake by this type of particle is restricted. For this reason, even though SO_4^{2-} particle population is much higher than Na particle population, the uptake rate of MSA-SO_4^{2-} particles is much lower than that of MSA-Na particles (Fig. 6).

The uptake rates of MSA-OC and MSA-NO_x^- particles are 0.37 ± 0.38 and 0.35 ± 0.62, respectively (Fig. 6). This is consistent with the relative abundances of MSA-OC and MSA-NO_x^- particles and the corresponding OC and NO_x^- particles (Fig. 4). It indicates that the uptake rates of MSA on existing particles are determined by the aerosol properties, alkaline sea salt particles enhance the uptake of MSA, while acidic and hydrophobicity species suppress the uptake of MSA on these particles.

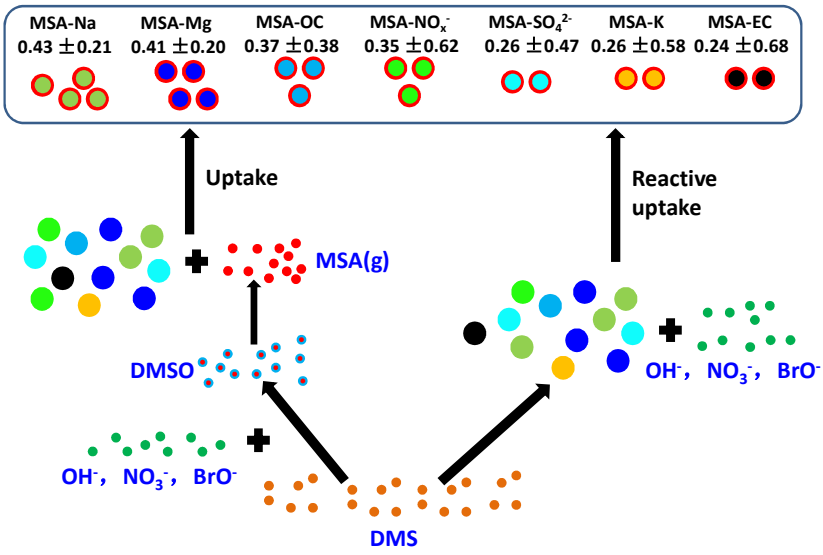

Fig. 6 MSA uptake rates on different aerosol particles in the marine atmosphere.

4. Conclusions

The uptake characteristics of MSA on different aerosols were examined during the early December 2017 and January-February 2018 in the polynya regions of the RS, Antarctica. Particulate MSA mass concentration, as well as particle populations and size distributions, were determined simultaneously for the first time to characterize the formation of MSA on different particles. To access the interactions between MSA and other species, MSA particles were classified into seven sub-types using the ART-2a algorithm: MSA-Na, MSA-Mg, MSA-SO_4^{2-}, MSA-K, MSA-EC, MSA-OC, and MSA-NO_x^-.

MSA mass concentration do not always reflect MSA particle population in the marine atmosphere. MSA uptake occurred on aerosol surfaces alters the aerosol size and chemical compositions, but do not change the aerosol population. MSA particle population is mainly associated with the total particle population, as more particles implies a greater opportunity for MSA uptake. High MSA mass concentrations with low MSA populations occur, when low existing particle population with high MSA production from the oxidation of DMS are present.

The uptake of MSA on existing particles is mainly dependent on aerosol properties. Alkaline sea salt particles enhance the uptake of MSA, as high uptake rates of MSA-Na and MSA-Mg particles are observed in the Na and Mg particles, accounting for 0.43 ± 0.21 and 0.41 ± 0.20 of

the total Na and Mg particles, respectively. But acidic and hydrophobicity species suppress the uptake of MSA on these particles, as only 0.24 ± 0.68 and 0.26 ± 0.47 of MSA-EC and MSA-SO_4^{2-} are present in the total EC and SO_4^{2-} particles. The results extend the knowledge of the impact of aerosol properties on the conversion of MSA in the marine atmosphere, however, the details of the formation of MSA are complicated and still controversial. Observations and especially simulation experiments in the laboratory are required in the future to clarify the formation of MSA and their impact factors in the marine atmosphere.

Code and Data availability.

The data used in the figures, as well as the time series of the cruise tracks, MSA mass concentration and particle mass concentrations obtained from the IGAC, MSA particle population, size distribution and mass spectra obtained from the SPAMS, as well as wind speeds and directions, temperature and RH, are available at https://doi.org/10.5281/zenodo.3614694 (Jinpei Yan, 2020). Codes for the analysis are available from JP upon request.

Author contributions.

JY conducted the observations, analyzed the results, and wrote the paper. JJ contributed the data analyses and paper writing. MZ conducted the on-board observations. FB and YT contributed to the refining the ideas and contributed considerably to the interpretation of the results. SX and SZ applied the calculations of sea ice distribution and Metrological data. QL and LL contributed the observation data analyses. LC and JY were together responsible for the design of the study. All authors were involved in discussing the results and improved the paper by proofreading.

Competing interests.

The authors declare that they have no conflict of interest.

Acknowledgements

The authors gratefully acknowledge Guangzhou Hexin Analytical Instrument Company Limited for the SPAMS data analysis and on-board observation technical assistance, and Zhangjia Instrument Company Limited (Taiwan) for the IGAC technical assistance and data analysis. We would like to thank Meijiao Pang for the SPAMS maintenance on-board during the cruise.

Financial support

This study is Financially Supported by Qingdao National Laboratory for marine science and technology (No. QNLM2016ORP0109), the Natural Science Foundation of Fujian Province, China (No. 2019J01120), the National Natural Science Foundation of China (No. 41941014). Jinyoung Jung was supported by grants from Korea Polar Research Institute (KOPRI) (PE20140).

References

Adachi, K., Buseck, P. R. Changes in shape and composition of sea-salt particles upon aging in an urban atmosphere. Atmos. Environ. 100, 1-9, 2015.

Allen, J.O. YAADA: Software Toolkit to Analyze Single-Particle Mass Spectral Data, 2005.

Ayers, G.P., Cainey, J.M., Gillett, R.W., Ivey, J.P. Atmospheric sulphur and cloud condensation nuclei in marine air in the Southern Hemisphere, Phil. Trans. R. Soc. Lond. B, 352, 203-211, 1997.

Barnes, I., Hjorth, J., Mihalopoulos, N. Dimethyl sulfide and dimethyl sulfoxide and their oxidation in the atmosphere. Chem. Rev. 106, 940-975, 2006

Bardouki, H., Berresheim, H., Erkoussis, M., Sciare, J., Kouvarakis, G., Oikonomou, K., Schneider, J., Mihalopoulos, N. Gaseous (DMS, MSA, SO2, H2SO4 and DMSO) and particulate (sulphate and methanesulfonate) sulphur species over the northeastern coast Crete. Atmos. Chem. Phys. 3, 1871-1886, 2003.

Bates, T. S., Calhoum, J. A., Quinn, P. K. Variations in the methane sulphonate to sulphate molar ratio in submicrometer marine aerosol particles over the South Pacific Ocean. J. Geophys. Res. 97, 9859-9865, 1992.

Bork, N., Elm, J., Olenius, T., Vehkamaki. Methane sulfonic acid-enhanced formation of molecular clusters of sulfuric acid and dimethyl amine. Atmos. Chem. Phy. 14, 12023-12030, 2014.

Casillas-Ituarte, N.N., Callahan, K. M., Tang, C.Y., Chen, X., Roeselova, M. Surface organization of aqueous MgCl2 and application to atmospheric marine aerosol chemistry. PNAS, 107, 6616-6621, 2010.

Cavalieri, D. J., and Parkinson, C. L. 30-Year satellite record reveals contrasting Arctic and Antarctic decadal sea ice variability. Geophys. Res. Lett. 30(18), 2003.

Chang, R. Y.-W., Sjostedt, S. J., Pierce, J. R., Papakyriakou, T. N., Scarratt, M. G., Michaud, S., et al. Relating atmospheric and oceanic DMS levels to particle nucleation events in the Canadian Arctic. J. Geophys. Res. 116, D00S03, 2011.

Chen, L., Wang, J., Gao, Y., Xu, G., Yang, X., Lin, Q., Zhang, Y. Latitudinal distributions of atmospheric MSA and MSA/nss-SO42- ratios in summer over the high latitude regions of the Southern and Northern Hemispheres. J. Geophys. Res. 117, D10306, 2012.

Clarke, A. D., Owens, S. R. Zhou, J. An ultrafine sea-salt flux from breaking waves: implications for cloud condensation nuclei in the remote marine atmosphere. J. Geophys. Res. 111, D06202. (doi:10.1029/2005JD006565), 2006.

Davis, D., Chen, G., Kasibhatla, P., Jefferson, A., Tanner, D., Eisele, F., Lenschow, D., Neff, W., Berresheim, H. DMS oxidation in the Antarctic marine boundary layer: Comparison of model simulations and field observations of DMS, DMSO, $DMSO_2$, $H_2SO_4(_g)$, $MSA(_g)$, and $MSA(_p)$. J. Geophys. Res. 103, 1657-1678, 1998.

De Baar, H. J., De Jong, J. T., Bakker, D. C., Löscher, B. M., Veth, C., Bathmann, U., Smetacek, V. Importance of iron for plankton blooms and carbon dioxide drawdown in the Southern Ocean. Nature, 373, 412-415, 1995.

De Leeuw, G., Andreas, E. L, Anguelova, M. D., Fairall, C. W., Lewis, E. R., O'Dowd, C., Schulz, M., and Schwartz, S. E. Production flux of sea spray aerosol, Rev Geophys., 49, RG2001, doi:10.1029/2010RG000349, 2011.

Gaston, C.J., Furutani, H., Guazzotti, S. A., Coffee, K.R., Bates, T.S., Quinn, P.K., Aluwihare, L.I. Mitchell, B.G., Prather, K. Unique ocean-derived particles serve as a proxy for changed in ocean chemistry. Journal of Geophysical Research, 116, D18310, 2011

Guazzotti, S. A., Coffee, K. R., Prather K. A. Continuous measurements of size‐resolved particle chemistry

during INDOEX Intensive Field Phase 99, J. Geophys. Res., 106(D22), 28,607 – 28,627, doi:10.1029/2001JD900099, 2001.

Ghahremaninezhad, R., Norman, A.-L., Abbatt, J. P. D., Levasseur, M., Thomas, J. L. Biogenic, anthropogenic and sea salt sulfate size-segregated aerosols in the Arctic summer. Atmos. Chem. Phy. 16, 5191-5202, 2016.

Hayashida, H., Steiner, N., Monahan, A., Galindo, V., Lizotte, M., Levasseur, M. Implications of sea-ice biogeochemistry for oceanic production and emissions of dimethyl sulfide in the Arctic. Biogeosciences. 14, 3129-3155, 2017.

Healy, R. M., Hellebust, S., Kourtchev, I., Allanic, A., O'Connor, I. P., Bell, J. M., Healy, D. A., Sodeau, J. R., Wenger, J. C. Source apportionment of $PM_{2.5}$ in Cork Harbour, Ireland using a combination of single particle mass spectrometry and quantitative semi-continuous measurements. Atmos. Chem. Phy. 10, 9593-9613, 2010.

Horne, J.R., Zhu, S., Montoya-Aguilera, J., Hinks, M.L., Wingen, L.M., Nizkorodov, S.A., Dabdub,D. Reactive uptake of ammonia by secondary organic aerosols: Implications for air quality. Atmos. Environ. 189, 1-8, 2018.

Jung, J., Furutani, H., Uematsu, M., Park, J.. Distributions of atmospheric non-sea-salt sulfate and methanesulfonic acid over the Pacific Ocean between 48°N and 55°S during summer. Atmos. Environ. 99, 374-384, 2014.

Kloster, S., Feichter, J., Maier-Reimer, E., Six, K. D., Stier, P., Wetzel, P. DMS cycle in the marine ocean-atmosphere system? a global model study. Biogeosciences, 3, 29-51, 2006.

Laskin, A., Gaspar, D.J., Wang, W., Hunt, S. W., Cowin, J.P., Colson, S.D., Finlayson-Pitts, B.J. Reactions at interfaces as a source of sulfate formation in sea-salt particles. Science, 301(5631), 340-344, 2003.

Legrand, M., Pasteur, E. C. Methane sulfonic acid to non-sea-salt sulfate ratio in coastal Antarctic aerosol and surface snow. J. Geophys. Res. 103, 10991-11006, 1998.

Li, L., Huang, Z., Dong, J., Li, M., Gao, W., Nian, H., Fu, Z., Zhang, G., Bi, X., Cheng, P., Zhou, Z. Real time

509 bipolar time-of-flight mass spectrometer for analyzing single aerosol particles. Int. J. Mass Spectrom. 303,
510 118-124, 2011.
511 Li, L., Li, M., Huang, Z.X., Gao, W., Nian, H.Q., Fu, Z., Gao, J., Chai, F.H., Zhou, Z. Ambient particle
512 characterization by single particle aerosol mass spectrometry in an urban area of Beijing. Atmos. Environ. 94,
513 323-331, 2014.
514 Liu, M., Song, Y., Zhou, T., Xu, Z., Yan, C., Zheng, M., Wu, Z., Hu, M., Wu, Y., Zhu, T. Fine particle pH during
515 severe haze episodes in northern China, Geophys. Res. Lett. 44, 5213-5221, 2017.
516 Lizotte, M. P. The Contributions of Sea Ice Algae to Antarctic Marine Primary Production. Am. Zool. 41, 57-73,
517 2001.
518 Loose, B., Miller, L. A., Elliott, S., Papakyriakou, T. Sea ice biogeochemistry and material transport across the
519 frozen interface. Oceanography, 24, 202-218, 2011.
520 Mazzera, D. M., Lowenthal, D. H., Chow, J. C., Watson, J. G. Sources of PM_{10} and sulfate aerosol at McMurdo
521 Station, Antarctica. *Chemosphere*, 45, 347-356, 2001.
522 Minikin, A., Legrand, M., Hall, J., Wagenbach, D., Kleefeld, C., Wolff, E., Pasteur, E. C., Ducroz, F.
523 Sulfur-containing species (sulfate and methanesulfonate) in coastal Antarctic aerosol and precipitation, J.
524 Geophys. Res., 103, 10975-10990, 1998.
525 Murphy, S. M., Agrawal, H., Sorooshian, A., Padró, L.T., Gates, H., Hersey, S. Comprehensive simultaneous
526 shipboard and airborne characterization of exhaust from a modern container ship at sea. Environ. Sci. Tech.
527 43, 4626-4640, 2009.
528 Norris, S. J., Brooks, I. M., Moat, B. I., Yelland, M. J. Near-surface measurement of sea spray aerosol production
529 over whitecaps in the open ocean. Ocean Sci. 9, 133-145, 2013.
530 Pant, V., Siingh, D., Kamra, A.K., Size distribution of atmospheric aerosols at Maitri, Antarctica. Atmospheric

Environment, 45, 5138-5149, 2011.

Prather, K.A., Bertram T.H., Grassian V.H., Deane G.B., Stokes M.D., DeMott P.J., Aluwihare L.I., Palenik B.P., Azam, F. Seinfeld J.H., Moffet, R.C., Molina, M.J., Cappa, C.D., Geiger, F.M., Roberts, G.C., Russell, L.M., Ault, A.P., Baltrusaitis, J., Collins, D.B., Corrigan, C.E., Cuadra-Rodriguez, L.A., Ebben, C.J., Forestieri, S.D., Guasco, T.L., Hersey, S.P., Kim, M.J., Lambert, W.F., Modini, R.L., Mui, W., Pedler, B.E., Ruppel, M.J., Ryder, O.S., Schoepp, N.G., Sullivan, R.C., Zhao D. Bringing the ocean into the laboratory to probe the chemical complexity of sea spray aerosol. PNAS, 110(19):7550-7555, 2013.

Preunkert, S., Jourdain, B., Legrand, M., Udisti, R., Becagli, S., Cerri, O. Seasonality of sulfur species (dimethyl sulfide, sulfate, and methanesulfonate) in Antarctica: Inland versus coastal regions. J. Geophys. Res. 113, D15302, 2008.

Preunkert, S., Legrand, M., Jourdain, B., Moulin, C., Belviso, S., Kasamatsu, N., Fukuchi, M., Hirawake, T. Interannual variability of dimethylsulfide in air and seawater and its atmospheric oxidation by-products (methanesulfonate and sulphate) at Dumont d'Urville, coastal Antarctica (1999-2003). J. Geophys. Res. 112, 2007.

Quinn, P.K., Coffman, D.J., Johnson, J.E., Upchurch, L.M., Bates, T.S. Small fraction of marine cloud condensation nuclei made up of sea spray aerosol, Nature Geoscience, doi:10.1038/NGEO3003, 2017.

Quinn, P.K., Bates, T.S., Schulz, K.S., Coffman, D.J., Frossard, A.A., Russell, L.M., Keene, W.C., Kieber, D.J. Contribution of sea surface carbon pool to organic matter enrichment in sea spry aerosol. Nature Geos. 7, 228-232, 2014.

Read, K. A., Lewis, A. C., Bauguitte, S., Rankin, A. M., Salmon, R. A., Wolff, E. W., Saiz-Lopez, A., Bloss W. J., Heard, D. E., Lee, J. D., Plane, J. M. C. DMS and MSA measurements in the Antarctic Boundary Layer: impact of BrO on MSA production. Atmos. Chem. Phys. 8, 2985-2997, 2008.

553 Savoie, D.L., Prospero, J.M., Larsen,R.J., Huang, F., Izaguirre, M.A., Huang, T., Snowdon, T.H., Custals, L.,
554 Sanderson, C.G. Nitrogen and sulfur species in Antarctic aerosols at Mawson, Palmer, and Marsh (King
555 George Island), J. Atmos. Chem. 17, 95-122, 1993.
556 Schlitzer, R. Ocean Data View, Odv.awi.de, 2015.
557 Schlitzer, R. Interactive analysis and visualization of geosciences data with Ocean Data view. Comput. Geosci. 28,
558 1211–1218, 2002.
559 Song, X.H., Hopke, P.K., Fergenson, D.P., Prather, K.A. Classification of single particles analyzed by ATOFMS
560 using an artificial neural network, ART-2A. Analy. Chem. 71, 860-865, 1999.
561 Sorooshian, A., Lu, M. L., Brechtel, F. J., Jonsson, H., Feingold, G., Flagan, R.C., Seinfeld, J.H. On the source of
562 organic acid aerosol layers above clouds. Environ. Sci. Technol. 41, 4647-4654, 2007.
563 Spreen, G., Kaleschke, L., and Heygster, G. Sea ice remote sensing using AMSR-E 89 GHz channels, J. Geophys.
564 Res., 113, C02S03, 2008.
565 Silva, P. J., Carlin, R. A., Prather, K. A. Single particles analysis of suspended soil dust from Southern California.
566 Atmos. Environ. 34, 1811-1820, 2000.
567 Sitaras, I. E., Siskos, P. A. The role of primary and secondary air pollutants in atmospheric pollution: Athens urban
568 area as a case study. Environ. Chem. Lett. 6, 59-69, 2008.
569 Tao, J., Zhang, Z., Tan, H., Zhang, L., Wud, Y., Sun, J., Chee, H., Cao, J., Cheng, P., Chen, L., Zhang, R.
570 Observation evidence of cloud processes contributing to daytime elevated nitrate in an urban atmosphere.
571 Atmos. Environ. 186, 209-215, 2018.
572 Taylor, M. H., Losch, M., Bracher, A. On the drivers of phytoplankton blooms in the Antarctic marginal ice zone:
573 A modeling approach. J. Geophys. Res. 118, 63-75, 2013.
574 Teinila, K., Frey, A., Hillamo, R., Tulp, H. C., Weller, R. A study of the sea-salt chemistry using size-segregated

aerosol measurements at coastal Antarctic station Neumayer. Atmos. Environ. 96, 11-19, 2014.

Tian, M., Wang, H., Chen, Y., Zhang, L., Shi, G., Liu, Y., Yu, J., Zhai, C., Wang, J., Yang, F. Highly time-resolved characterization of water-soluble inorganic ions in PM2.5 in a humid and acidic mega city in Sichuan Basin, China. Sci. Total Environ. 580, 224-234, 2017.

Wang, S., Bailey, D., Lindsay, K., Moore, J. K., Holland, M. Impact of sea ice on the marine iron cycle and phytoplankton productivity. Biogeosciences, 11, 4713-4731, 2014.

Weller, R., Legrand, M., Preunkert, S. Size distribution and ionic composition of marine summer aerosol at the continental Antarctic site Kohnen. Atmos. Chem. Phys., 18, 2413-2430, 2018.

Wolff, E. Nitrate in polar ice, in Ice Core Studies of Global Biogeochemical Cycles, edited by R. Delmas, Springer-Verlag, New York, 195-224, 1995.

Yan, J., Lin, Q., Zhao, S., Chen, L., Li, L. Impact of marine and continental sources on aerosol characteristics using an on-board SPAMS over Southeast Sea, China. Environ. Sci. Pollution Res. 25, 30659-30670, 2018.

Yan, J., Chen, L., Lin, Q., Li, Z., Chen, H., Zhao, S. Chemical characteristics of submicron aerosol particles during a long-lasting haze episode in Xiamen, China. *Atmos. Environ.* 113, 118-126, 2015.

Young, L. H., Li, C. H., Lin, M. Y., Hwang, B. F., Hsu, H. T., Chen, Y. C., Jung, C. R., Chen, K. C., Cheng, D. H., Wang, V. S., Chiang, H. C., Tsai, P. J. Field performance of semi-continuous monitor for ambient PM2.5 water-soluble inorganic ions and gases at a suburban site. Atmos. Environ. 144,376-388, 2016.

Zhang, M., Chen, L., Xu, G., Lin, Q., Liang, M. Linking phytoplankton activity in polynyas and sulfur aerosols over Zhongshan Station, East Antarctica. J. Atmos. Sci. 72, 4629-4642, 2015.